

## Cell Segmentation Comprehensive Algorithm in 3D Microscopic Images Based on Inverse Wavelet Transform

<sup>1</sup>Vahid Khodadadi, <sup>2</sup>Morteza Behnam Pooyan and <sup>2</sup>Alinaghi Hosseinabadi

<sup>1</sup>Department of Biomedical Engineering, Islamic Azad University,  
Science and Research Branch, Tehran, Iran

<sup>2</sup>Department of Electrical Engineering, Islamic Azad University,  
Najafabad Branch, Najafabad Isfahan, Tehran, Iran

---

**Abstract:** The correct and detailed segmentation of cells are very critical for cellular dynamic observation in biologic. The provided novel algorithm Cell Segmentation Comprehensive Algorithm (CSCA) is a comprehensive and full automatic without away type and number of cells limitation for segmentation based on a novel method by inverse wavelet transform. In our algorithm, first 3D image slices are preprocessing separately. Then every noise slice is decreased by passing off a BM3D filter with optimum parameters. So, after histogram equalization in every slice image, we decreased the image background by a new method that passing in parallel of different Gaussian filter and subtract two images filtered by Gaussian filter. Then in the next stage, the object edges are recognized by using Gradient Vector Flow (GVF) and morphological operators, then corresponding novel formula with image structure data is used for omitting the picture omissions. Finally, by applying 2D wavelet transform from each slice, every four components of 2D wavelet transform in a matrix are stored separately and after processing of all slices and saving in four 3D matrixes. Then, it is converted to 3D image by using 3D inverse wavelet transform in four matrixes. Finally, we detect and segment all of the cells that are inside or interface of frames 3D as a visual frame. The given algorithm on data has been tested with accuracy rate of 97.22%.

**Key words:** Segmentation, GVF, BM3D, inverse wavelet transform, local otsu, structure local

---

### INTRODUCTION

Cellular dynamics is a very important science in biology which, deals with cells driving force and its changes. Cells movement from one place to one there and the changes during cell activity is called cellular dynamics. One of the cell dynamic introductions is optimized segmentation. One of the cell segmentation algorithm applications is studying and reviewing cells behaviour. The main applications of segmentation algorithms are searching in cells, effecting a drug on shape of them or studying chemical or electrical effect on shape of cells. For example, researcher would like to see, how steam cell changes to neuron cell or other cell. In recent years, most of science molecular laboratory specialists are studying many of sequential frames for the cellular dynamic process by eyes which is a time consuming, boring and high error process. Also if, there is a lot of image for searching and studying in shape of cell, it is impossible. Of course, some algorithms are presented up to now but each of them has some

limitations such as cell counts or cell type in circular or solar shape. Also many of these algorithms are semi-automatic or fully automatic for one type of cell. There are many algorithms for segmentation in 2D and 3D that we introduce some of them. One method of segmentation is based on level set deformable model and convex minimization. Indeed, they used different convex energy function, based on the efficient numeric method for minimization and integrated a shape for the cell (Bergeest and Rohr, 2014). Another, method is a semi-automatic algorithm which by configuration image properties, segment convex structure of growing local region (Pfister *et al.*, 2013). Some techniques are used in tracking algorithm for segmentation such as usage largest areas connected to each image or morphological operation for segmentation (Meyer and Beucher, 1990). By using a compound method, middle filter and morphological operators such as erosion and dilation has accomplished this segmentation (Anoraganingrum, 1999) or in another method, the segmentation is carried out by a simple wavelet transform with the level-set algorithm (Yang and

Padfield, 2009). An algorithm is used for white blood cell segmentation as well which the image was first used by a scale-space filtering for recognition and extraction of cell core. Then watershed clustering in 3D HSV histogram was proposed to extract cytoplasm region.

Finally, morphological operators were used for connective regions (Jiang *et al.*, 2003). Obtaining same of give Algorithm, have employed segmentation based on an unsupervised GVF snake. In fact, they used a convex hull as on early contour for cell recognition. Also, a pixel classification is used which trained a set of Bayesian classification from cluster local training image patches (Yin *et al.*, 2010). HIS colour space method was used for segmentation indeed they used S and H information which each one has some properties have carried out the segmentation by using OTSU and circular histogram method. Another method which is using adaptive thresholding and watershed is based on trend and no trend feature with Markov model (Zhou *et al.*, 2009) or using a sliding bond filter algorithm, this filter is used to make it adequate to segment overall convex shape and as such it performs well for cell detection. Also, the parameters involved are intuitive as they are directly related to expected cell size (Quelhas *et al.*, 2010). It is generally said that in recent year there has been different algorithm for 3D cell segmentation in microscopic images which is based on thresholding approaches (Liao and Deng, 2002). and is used changes based on watershed (Sharif *et al.*, 2012; Cheng and Rajapakse, 2009; Yang *et al.*, 2006) or segmentation based on 2D radial voting to an efficient three dimension implementation and iterative radial voting at multiple cellular (Han *et al.*, 2011) and the dynamic programming approaches. Their segmentation begins by semi-automatic algorithm, two dimension cell detection in a user-selected plane, using dynamic programming to locate the boundary with an accumulated intensity per unit length greater than any other possible boundary around the same object. Then the two surfaces of the cell in planes above and below the selected map are detected using an algorithm that combines dynamic programming and combinatorial searching (McCullough *et al.*, 2008). Graph cut based approaches, graph cuts use to detect the globally optimal segmentation of the, also the user marks some pixels as cell or background of cell's image to present hard constraints for it or main class of cell segmentation based on a formable model which can capture a wide spectrum of different shape and allow incorporation of prior knowledge distinguish between parametric model and implicit models (Boykov and Jolly, 2001; Lin *et al.*, 2007; Maska *et al.*, 2013; Padfield *et al.*, 2009; Lin *et al.*, 2005) another algorithm is based on active surfaces, it describes a fully automatic segmentation and tracking method designed for active quantitative analyses of cell shape

and motion from dynamic 3D microscopy data. It uses multiple active surfaces with or without edges and a volume conservation constraint that repairs outlining of cell border (Dufour *et al.*, 2005). Other method is presented for segmentation based on gradient diffusion gradient flow tracking and grouping, then using a local adaptive thresholding (Li *et al.*, 2007). In another method, the signal to noise ratio of image is first repaired with an edge preserving filtering, so the cell boundary is reconstructed using a fully automated method based on a subjective surfaces technique (Zanella *et al.*, 2010). In another method, combining curvature information with a distance map is used for segmentation of cells and then their algorithm extracts correct markers corresponding to the nucleus of each cell. So, watershed segmentation for segmentation the nuclei is used (Zhang *et al.*, 2011). As it was said before, all algorithms have some limitation of number and type cells or as they were tested only on one type of cell, they have low accuracy. In this study, we will provide a novel and a fully automatic algorithm which doesn't have any type or count cell limitation and will perform segmentation with an acceptable accuracy.

## MATERIALS AND METHODS

**Proposed cell segmentation algorithm:** In our method, we presented a novel algorithm that is shown in Fig. 1. At first has been separated every slice of a 3D image. Then all of slices are processed by following method, at the end, we compact all of the slices of the image.

**BM3D filter:** Filter as our input image has some noises such as alternate noises, it is necessary to eliminate noise of these images before any preprocessing. In this study one of the most important words relates to microscopic image noise omission. In this method, the used 3D Block Matching filter (BM3D) has been employed for omitting Gaussian noise in every slice of image. The base of this algorithm is a repetition of similar areas of image in place areas and similar blocks accumulation and applying the transformation (Han *et al.*, 2011). In this filter, first the every slice of image for omitting noise is divided into two groups. It includes two primary and wiener filter stages. The primary stage includes three steps of.

**Primary filter:** The stage of Primary filter as the first procedure of our proposed scenario is carried out using three steps. These steps are as following:

- Grouping
- Hard threshold
- Aggregation

**Grouping:** In the first stage, the slice of image is converted into small blocks. The small blocks are 8×8. To

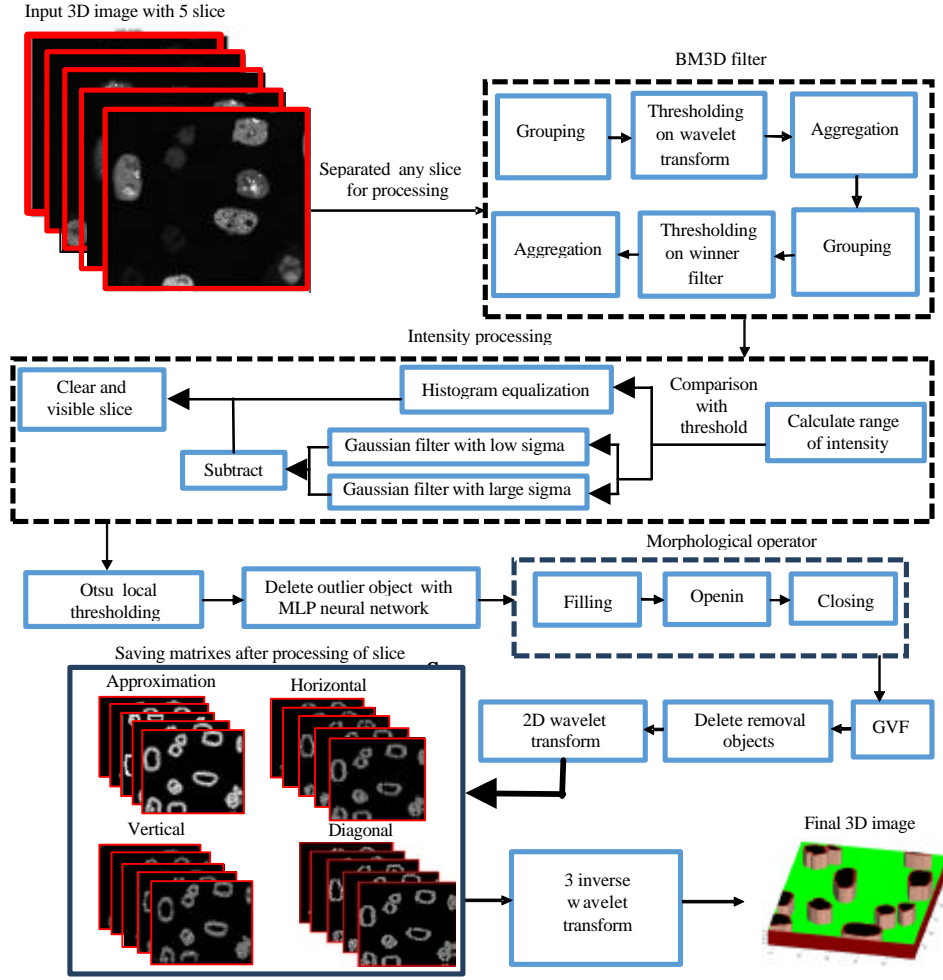


Fig. 1: Block diagram of cell segmentation comprehensive algorithm

compare the blocks, we choice the number of blocks as reference block. For choosing the reference block, the first block is put as the reference and other blocks are by 3 block distance. Each reference block is compared with 45 nearest blocks in the image. Also, for improvement of grouping at first, every block is passed of wavelet transform with Haar function. At last, all blocks of slice are grouped based on threshold by:

$$d^{\text{Noisy}}(B_{XR}, B_X) = \frac{|\Gamma(\Gamma_{2D}^{w,v}(B_{XR})) - \Gamma(\Gamma_{2D}^{w,v}(B_X))|^2}{(N)^2} \quad (1)$$

Where:

- N = The block length (block distance) in the primary stage
- $B_{XR}$  = Reference block

- $B_x$  = Noise image block in x position, respectively
- $\tilde{\Lambda}^{w,v}$  = Wavelet transform and
- T = A threshold for coefficients of wavelet transform
- T = Threshold is 2500
- $d^{\text{noisy}}$  = Value of similarity between reference block and noisy block (Han *et al.*, 2011)

So, we have many groups of blocks are grouped in 3D matrix based on the similarity.

**Hard thresholding:** So, a 3D transformation is applied on the multiple groups. The noise omission operation is performed by placing a hard threshold in this 3D wavelet transform. Then, it is accomplished inverse 3D transformation as:

$$d^{\text{basic}} = \Gamma_{3D}^{\text{wavelet}^{-1}}(T(\Gamma_{3D}^{\text{wavelet}}(d^{\text{noisy}}))) \quad (2)$$

Where:

- $d^{\text{basic}}$  = Groups that are omitted noise
- T = Threshold for coefficient of wavelet transform
- $\tilde{A}^{\text{wavelet}}$  = Wavelet transform with Biros function and
- $\tilde{A}^{\text{wavelet-1}}$  = Inverse of wavelet transform
- T = Threshold for coefficient of wavelet transform is 40.5

**Aggregation:** In aggregation stage, because of some blocks membership in different groups, there is the possibility of blocks overlapping. For solving this problem, the blocks are weighted by an estimated blocks achiever by Eq. 3. Weight averaging, so the noisier groups get less weight:

$$W = \begin{cases} \frac{1}{\sigma^2 * n} & n > 1 \\ 0 & \text{O. W} \end{cases} \quad (3)$$

Where:

- n = Sum of remaining non-zero coefficients
- $\sigma$  = Noise standard deviation that is 15

Now, after each pixel in every block is weighted, the estimated slice is achieved by weight (Yang and Padfield, 2014). So, every pixel that has lower weight in all of the blocks is selected as winner pixel. So, we have one slice again;

**Wiener filter:** And the wiener filter stage includes three steps of:

- Grouping
- Wiener filter
- Aggregation

**Grouping:** The second stage of BM3D filter is winner filter. In this stage, the grouping process is the same as former stage. But in this level the slice of the image has lower noise than previous level because we use 2 thresholds for omitting the noise.

**Wiener filter:** But in this stage is after grouping the slices in many groups of 3D matrix. So, for omitting a noise in slice of image and having a clear image, we placing wiener filter on each group coefficients is obtained as:

$$W_x = \frac{|\Gamma_{3D}^{\text{WIN}}(d_x)|^2}{|\Gamma_{3D}^{\text{WIN}}(d_x)|^2 + \sigma^2} \quad (4)$$

Where:

- d = Blocks grouped and
- $\tilde{A}^{\text{WIN}}$  = 3D winner transform in 3D matrix that are grouped

So, after doing 3D winner transform and thresholding on the coefficients of it, we can inverse 3D winner transform (Yang and Padfield, 2014). Therefore, the noise omission is performed by multiplying these weights by 3D noisy blocks coefficients finally, by doing 3D inverse transform, the noise omitting estimated blocks achiever as:

$$d_x^{\text{basic}} = \Gamma_{3D}^{\text{WIN-1}} \left( T \left( \Gamma_{3D}^{\text{WIN}} (W_x) \right) \right) \quad (5)$$

Where:

- $d^{\text{basic}}$  = 3D group that is omitted noise
- T = Threshold on coefficients winner transform
- $\Gamma$  = Coefficients winner transform is 400
- $\tilde{A}^{\text{WIN}} \tilde{A}^{\text{WIN-1}}$  = Winner transform and inverse transform

**Aggregation:** As before, in aggregation stage, there is error possibility because of selected blocks overlapping in all groups. For solving this problem, the pixels are weighted same. Finally, the noise omitting image pixels based on weight averaging are obtained. In this study, premium parameters are provided for using this algorithm. These parameters are achieved based on trial and error.

**Histogram equalization:** With studies on available 3D images on databases, we divided images into two groups: for dividing at first, histogram of slice is calculated so subtract minimum and maximum intensity of the histogram (Lin *et al.*, 2005; Zanella *et al.*, 2010).

Low intensity images which its objects or frame cells are not obvious. This image has subtracted <50. So, we must employ the histogram equalization procedure to show cells or object in slice. Also, this slice has clear cells than background after equalization.

Images with intensity >50. These available objects are obvious but the background effect have an intensity equal to cell intensity which make some problem in processing.

**Low pass gaussian filter with standard deviation of 3/8 and 42:** For clearing the slices that have threshold intensity >50, first two slices of original slices are zero padding delivered to fourier area (fourier transform), the resulting images in fourier area are passed through a low pass Gaussian filter with standard deviation of 3/8 and 42. Finally, the images are transformed into time domain and image dimension are transformed into a primary dimension with regard to zero padding. Of course it must be said, that filtering process is done on image if intensity difference is >50, otherwise only it is accomplished by histogram equalization

**Two filtered image difference:** Now we have two filtered images: one of them passing through a low pass Gaussian filter with sigma 3/8 and the other with sigma 42. So when it passed of Gaussian filter with sigma 3.8, it has a border

in boundary. By subtracting these two images, provided that filtered image with sigma 42 is doubled, we have an image with a low background effect and high foreground effect but with a border. This border will remove by following method.

**Thresholding:** The major problem with global thresholding is that we consider only the intensity, not any relationships between the cell's pixel and background. There is no guarantee that the pixels of cells identified by the thresholding process are contiguous. We can easily involve extraneous pixels that are not part of the desired region and we can just as easily miss isolated pixels within the region. These effects get worse as the noise gets worse, simply because it is more likely that pixels intensity doesn't represent the normal intensity in the region in 3D image. The 3D images have more sensitivity in binary action, so for transforming into binary image, we set aside global thresholding and used local with Otsu method. Otsu's thresholding method includes iterating through all the possible threshold values and calculating a measure of spread for the pixel levels each side of the threshold. Comparison between global thresholding and local thresholding shows how Otsu's threshold method can be applied locally. Local Otsu method is one of thresholding methods used in various fields images. The Two-dimensional Otsu method behaves well in segmenting images of low signal to noise ratio but it gives satisfactory results only when the numbers of pixels in each class are close to each other. So, local Otsu method for overcoming problem in our scenario is used. For each pixel, an optimal threshold is determined by maximizing the variance between two classes of pixels of the local neighborhood defined by a structuring element. The pixels that either fall in the foreground or background. The aim is to find the threshold value where the sum of foreground and background spreads is at its minimum. In fact, we define a rectangle with 40×40 pixel dimension and performed Thresholding process by Otsu method.

**Outlier data elimination:** We have a white background around each frame cells which must be eliminated. The white background is made by passing slice of Gaussian filter with standard division 3.8. For eliminating this effect we calculate all available objects area in the image. Now we recognized and eliminate the area which has the most difference of other object by neural network. At first we use a MLP neural network for detecting this outlier. Generally, we can consider data that have most difference of area mean of other object. Quorum of this difference

can consider with criterions like: Markov inequality and Chebyshev inequality but for using of Statistical Relations, we need a enough information about Probability Distribution Function (PDF) so we have to use methods based on a neural network. For deleting removal objects, area of some images are calculated and detected areas of cells to group: outlier and non-outlier. So by using a neural network Multilayer Perceptron (MLP) with Levenberg learning rule and Educational function of Back Propagation, data are classified in two groups. Number of neurons in the input neural network and preventing of over-fitting are set double numbers hidden layer. Ultimately, results of the MLP are categorized two perfect sets. Data have more difference area of another area and if have an acceptable MSE error are considered as a outlier and data are same together as desired data. Then by detecting object that is outlier in image, it is deleted.

**Image morphological operation:** It has been concluded that 3D cells have some cavities which includes cell components or nucleus. To eliminate this effect, all cavities in each area were filled. After filling any hole in the cells or objects, the cytoplasm of cells should be segmented. As available cells in some slices are connected to each other because of processing or even overlapping, even sometimes object frontier will open because of some removing these adverse effects. For separated cells are connected together we can use opening morphological but after opening we must use closing operator. Also for opening and closing, we must use a disk. But it related to detail of any frame, slice or type of cell. For selecting a disk with optimum radius, in every slice is calculated mean area of cells. After that is calculated mean of cell, it is selected as radius disc. So, the image is opened by a disc with radius mean which is the radius average of processing cells, so connected object separate and then again opened image will close with a mean radius disc. So, we in slice of image all of the hole is filled and connected cells are separated of together.

**Edge detection with GVF method:** In this method, an active function on slice is defined for segmentation which image edges are achieved by minimizing this that is the same energy function. For defining at first we must define edge function. Edge function is a vector of absolute gradient intensity profile in image and has 3 notes:

- Its vector toward an edge of cell or object in slice and perpendicular on edges
- Values of these vectors are very much in near of edges

- Value of these vectors are near two zero in inside or outside objects or cell

Therefore, after calculating gradient vector, we use an energy function. To be minimum this function, we can get edges by:

$$E = \iint \mu (u_x^2 + u_y^2 + v_x^2 + v_y^2) + |\nabla f|^2 |V - \nabla f|^2 \quad (6)$$

$$V(x, y) = [u(x, y), v(x, y)] \quad (7)$$

Where:

$\nabla$  = Edge function

$\mu$  = A coefficient and u and v is integrate toward x and y For obtaining the minimum function energy

E = It is calculated a function based on

V = So after calculating function

V = Any edge of objects in slice is detected

But when we detected edge object in slice, the objects are connected to border of image are not close ring and they must be close because for calculating areas on flowing are not calculate able [7]. So, we detected objects are connected to the border and are connected end and last point together.

**Data and objects elimination:** By looking at 3D processed images, the object elimination procedure is used. In our microscopic image there is a lot of redundancy objects that some of them are made when we are processing or some of them related to structure of tissue or blood when are imaged. There are many methods for deleting redundancy object in cells. But the oldest methods are not based upon the structural of cell or oldest methods are based on a type of cell. In this case, we present a new method that it can use for all type cells and it is fully automatic. We calculate object area and among these areas, these outlier data are redundant object in the image and it must be eliminated. Thresholding amount ( $S_{TH1}$ ) for eliminating small objects:

$$S_{TH1} = (2 \times S_{Min}) + S_{Mean} \quad (8)$$

$$S_{TH2} = (2 \times S_{Min}) + (2 \times S_{Mean}) \quad (9)$$

Where:

$S_{min}$  = Area minimum of cell or object in the slice and

$S_{mean}$  = Area mean of cell or objects

We calculated these formula based on experimental. So, if any object has area value less than  $S_{TH1}$  or has area value more than  $S_{TH2}$  it is detected as redundancy object and it deleted.

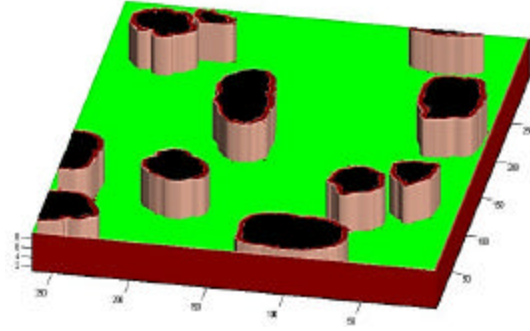


Fig. 2: A sample 3D image final after passing of Cell Segmentation Comprehensive Algorithm (CSCA)

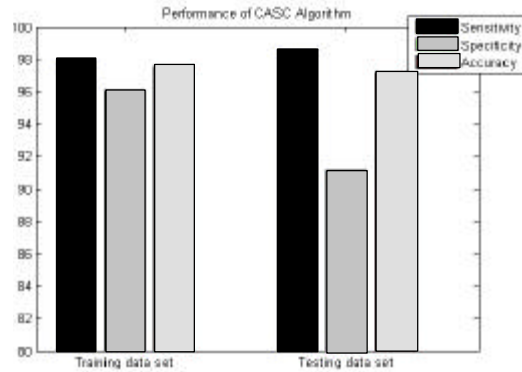


Fig. 3: Comparison between results of training and test

**Image reproduction based on 3d wavelet transform:** As it was said before, former processing operation set was done separately on each of 2D image slices. In this stage, after we separated any 3D image to 2D slice and they are processed one by one (Dufour *et al.*, 2005; Li *et al.*, 2007). Any slice at end passed with 2D wavelet transform with BiorSplines function and zero coefficient thresholding as four images with horizontal, vertical, diagonal details are the result of 2D wavelet transform of every slice. So, after that all of the slices are processed and passed of 2D wavelet transform and saving any four images are the results of 2D wavelet transform. Now we have four kinds of 3D matrices. So, at end we have four images matrix (horizontal, vertical, diagonal, details) are made by singles 2D wavelet (Dufour *et al.*, 2005). Now we use an inverse 3D wavelet transform on four 3D matrixes and we calculated one 3D image that are very clear and it has not any redundancy or removal object. For a prototype of our proposed scenario in image reproduction that relies on 3D wavelet transform, Fig. 2 is presented as a spectacle of this method. This Fig. 3 represents a sample result of our method that is called Cell Segmentation Comprehensive Algorithm (CSCA) in this study.

Table 1: Experimental results of testing and training of cell segmentation comprehensive algorithm

Parameters	Training dataset				Test dataset			
	TP	FP	FN	TN	TP	FP	FN	TN
Results of detection	1859	22	38	543	1992	41	28	423
Sensitivity (%)			97.99				98.61	
Specificity (%)	96.10		91.16					
Accuracy (%)	97.56		97.22					
No. of frames	364		364					
<b>Final results of CSCA</b>								
Validation Check (%)	94.11		Variance of error				0.057	
Mean of Accuracy (%)	97.39		Mean of error				2.61	

## RESULTS AND DISCUSSION

### Experimental results

**Image dataset:** In this study the dataset of cellular images is used. In this dataset includes three 3D image groups which have two groups for training and test. In general, the algorithm was trained by using a different 3D frames and was tested on different 3D frames.

The first group of cell is called N3DH-CHO, include two groups cell (training and test) that every group has 91 of 3D frames that every 3D frame has 5 slices 2D image. Also distance time between any 3D frames is 9.5 min and size of any 2D slice is 443×512. The second group of cell is called C3DH-H157, include two groups cell that every group has 59 of 3D frames that every 3D frame has 80 slices 2D image. Also, distance time between any 3D frames is 2 min and size of any 2D slice is 832×992. The first group of cell is called C3DL-MDA, include six groups cell that every group has 11 of 3D frames that every 3D frame has 30 slices 2D image. Also distance time between any 3D frames is 80 min and size of any 2D slice is 520×520.

**Final classification:** In this study, four main criterions are considered which include (TF, TP, FP and FN) and sensitivity, accuracy and precision rate to compare the results of our process, cells processed was seen as visually by a laboratory expert. These measures are attained as:

$$\text{Accuracy} = \frac{TP + TN}{P + N} \quad (10)$$

$$\text{Sensitivity} = \frac{TP}{TP + FN} \quad (11)$$

$$\text{Specificity} = \frac{TN}{FP + TN} \quad (12)$$

where, TP is numbers of cells that segmented with CSCA algorithm and it was approved by expert. FP is number of

Table 2: Comparison between our result and other results

Group name	Average of accuracy	RANK
COM-US	0.67	3
HEID-GE	0.65	4
KTH-SE	0.77	2
LEID-NL	0.89	1
PRAG-CZ	0.58	5
UPM-ES	NA	6
CSCA (our method)	0.97	-

cells that segmented with CSCA algorithm and it was not approved by expert. Also they are detected as redundancy objects by expert. FN is cells that were not segmented by CSCA algorithm or detected as removal objects and it was not approved by expert, also it is detected as cells by expert. TN is cells that are segmented with CSCA algorithm and it was approved by expert. The cells classification is applied by considering 400 frames as the test data and 400 different frames as the training set. For comparing of result of cell, all of the images are processed are checked by expert imaging in microscopic image. The results of cell identification are shown in Table 1.

**Comparison with other method:** In the challenge, six groups registered. Also our result and their results of them are shown in Table 2.

## CONCLUSION

As it was seen, our given algorithm does not have any type and count cell limitation. On each slice, a useful objects in said the images are deleted based on the slice information. However, in previous methods there were some limitation in automatic number of cells or some of them had very low accuracy, only incorporated on cell type. Our given algorithm incorporated all kinds of cells. In recent year, many algorithms have been provided which each of them had some limitations. In this study, we showed that if a noise omission method and ideal background effect omission is used, the best image segmentation is achieved by using and edge finder based on gradient. So, if we use filters are based random noise omitted and wavelet transform and reduce effect of

background of image, it has clear and visible image. Also, with comparing result of our algorithm with other algorithms, it is clear that methods are based on gradient vector flow have better results for edge detection. Also, for deleting all of redundancy objects in microscopic image, the best methods are based on structural information of image. So at end for computing final image after processing any slice, one of the best methods is inverse wavelet transform. So experimental result show CSCA have acceptable accuracy for segmentation.

#### ACKNOWLEDGEMENTS

Researchers would like to thank Science and Research Branch Islamic Azad University and Dr. Emad Fatemizade and Dr. Kamaledin Setarehdan. Also, would like to thank of managers of competition challenge 2012 for their dataset.

#### REFERENCES

- Anoraganingrum, D., 1999. Cell segmentation with median filter and mathematical morphology operation. Proceedings of the IEEE International Conference on Image Analysis and Processing, Sept. 27-29, Venice, Italy, pp: 1043-1046.
- Bergeest, J.P. and K. Rohr, 2014. Segmentation of cell nuclei in 3D microscopy images based on level set deformable models and convex minimization. Proceedings of the 2014 IEEE 11th International Symposium on Biomedical Imaging (ISBI), April 29-May 2, 2014, IEEE, New York, USA., ISBN:978-1-4673-1960-7, pp: 637-640.
- Boykov, Y.Y. and M.P. Jolly, 2001. Interactive graph cuts for optimal boundary region segmentation of objects in ND images. Proceedings of the Eighth IEEE International Conference on Computer Vision, 2001 ICCV, July 7-14, 2001, IEEE, New York, USA., ISBN:0-7695-1143-0, pp: 105-112.
- Cheng, J. and J.C. Rajapakse, 2009. Segmentation of clustered nuclei with shape markers and marking function. IEEE. Trans. Biomed. Eng., 56: 741-748.
- Dufour, A., V. Shinin, S. Tajbakhsh, A.N. Guillen and M.J.C. Olivo, *et al.*, 2005. Segmenting and tracking fluorescent cells in dynamic 3D microscopy with coupled active surfaces. IEEE. Trans. Image Process., 14: 1396-1410.
- Han, J., H. Chang, Q. Yang, G. Fontenay and T. Groesser, *et al.*, 2011. Multiscale iterative voting for differential analysis of stress response for 2D and 3D cell culture models. J. Microsc., 241: 315-326.
- Jiang, K., Q.X. Jiang and Y. Xiong, 2003. A novel white blood cell segmentation scheme using scale-space filtering and watershed clustering. Mach. Learning Cybernetics, 5: 2820-2825.
- Li, G., T. Liu, A. Tarokh, J. Nie and L. Guo, *et al.*, 2007. 3D cell nuclei segmentation based on gradient flow tracking. BMC Cell Boil., 8: 1-40.
- Liao, Q. and Y. Deng, 2002. An accurate segmentation method for white blood cell images. Proceedings of the 2002 IEEE International Symposium on Biomedical Imaging, July 7-10, USA., pp: 245-248.
- Lin, G., M.K. Chawla, K. Olson, C.A. Barnes and J.F. Guzowski, *et al.*, 2007. A multi model approach to simultaneous segmentation and classification of heterogeneous populations of cell nuclei in 3D confocal microscope images. Cytometry Part A, 71: 724-736.
- Lin, G., M.K. Chawla, K. Olson, J.F. Guzowski and C.A. Barnes *et al.*, 2005. Hierarchical, model based merging of multiple fragments for improved three dimensional segmentation of nuclei. Cytometry Part A, 63: 20-33.
- Maska, M., O. Danek, S. Garasa, A. Rouzaut and B.A. Munoz *et al.*, 2013. Segmentation and shape tracking of whole fluorescent cells based on the Chan Vese model. IEEE. Trans. Med. Imaging, 32: 995-1006.
- McCullough, D.P., P.R. Gudla, B.S. Harris, J.A. Collins and K.J. Meaburn, *et al.*, 2008. Segmentation of whole cells and cell nuclei from 3-D optical microscope images using dynamic programming. IEEE Trans. Med. Imaging, 27: 723-734.
- Meyer, F. and S. Beucher, 1990. Morphological segmentation. J. Visual Commun. Image Represent., 1: 21-46.
- Padfield, D., J. Rittscher, N. Thomas and B. Roysam, 2009. Spatio temporal cell cycle phase analysis using level sets and fast marching methods. Med. Image Anal., 13: 143-155.
- Pfister, S.S., M. Betizeau, C. Dehay and R. Douglas, 2013. Robust 3D cell segmentation by local region growing in convex volumes. Proceedings of the 2013 IEEE 10th International Symposium on Biomedical Imaging, April 7-11, 2013, IEEE, New York, USA., ISBN:978-1-4673-6456-0, pp: 426-431.
- Quelhas, P., M. Marcuzzo, A.M. Mendonca and A. Campilho, 2010. Cell nuclei and cytoplasm joint segmentation using the sliding band filter. IEEE. Trans. Med. Imaging, 29: 1463-1473.



- Sharif, J.M., M.F. Miswan, M.A. Ngadi, M.S.H. Salam and A.J.M. Bin, 2012. Red blood cell segmentation using masking and watershed algorithm: A preliminary study. Proceeding of the 2012 International Conference on Biomedical Engineering (IcoBE), February 27-28, 2012, IEEE, New York, USA., ISBN:978-1-4577-1989-9, pp: 258-262.
- Yang, X. and D. Padfield, 2014. Wavelet initialized 3D level-set cell segmentation with local background support. Proceedings of the 2014 IEEE 11th International Symposium on Biomedical Imaging (ISBI), April 29-May 2, 2014, IEEE, New York, USA., ISBN:978-1-4673-1960-7, pp: 814-817.
- Yang, X., H. Li and X. Zhou, 2006. Nuclei segmentation using marker controlled watershed, tracking using mean-shift and Kalman filter in time-lapse microscopy. IEEE. Trans. Circuits Syst. Regul. Pap., 53: 2405-2414.
- Yin, Z., R. Bise, M. Chen and T. Kanade, 2010. Cell segmentation in microscopy imagery using a bag of local Bayesian classifiers. Proceedings of the 2010 IEEE International Symposium on Biomedical Imaging: From Nano to Macro, April 14-17, 2010, IEEE, New York, USA., ISBN:978-1-4244-4126-6, pp: 125-128.
- Zanella, C., M. Campana, B. Rizzi, C. Melani and G. Sanguinetti *et al.*, 2010. Cells segmentation from 3D confocal images of early zebrafish embryogenesis. IEEE. Trans. Image Process., 19: 770-781.
- Zhang, C., Sun, C. and T.D. Pham, 2011. Clustered nuclei splitting using curvature information. Proceedings of the 2011 International Conference on Digital Image Computing Techniques and Applications (DICTA), December 6-8, 2011, IEEE, New York, USA., ISBN:978-1-4577-2006-2, pp: 352-357.
- Zhou, X., F. Li, J. Yan and S.T. Wong, 2009. A novel cell segmentation method and cell phase identification using Markov model. IEEE. Trans. Inf. Technol. Biomed., 13: 152-157.